OPEN

Vascular endothelial growth factor A induces proliferation of adult neural progenitor cells in non-neurogenic periventricular regions of the adult mouse hindbrain

Mareike Fauser[a,*], Roy Bockholt[b,c,*], Silke Keiner[d], Grit Weselek[a], Andreas Hermann[e,f,g], Christoph Redecker[h] and Alexander Storch[a,e,g]

Background **In addition to the well-established neurogenic niche of the ventricular-subventricular zone (V-SVZ) of the lateral ventricles, neural stem/progenitor cells (NPCs) have been identified in the periventricular regions (PVRs) throughout the adult mouse ventricular system. The potential role of these NPCs in neuroplasticity or neurorestoration, however, remains largely unexplored.**

Objective **Given that vascular endothelial growth factor A (VEGF-A) has been shown to promote stem cell proliferation in the V-SVZ, this study aimed to investigate VEGF-A effects on NPC proliferation in mid- and hindbrain PVRs.**

Methods **Healthy adult male C57BL/6 mice received continuous intracerebroventricular infusions of VEGF-A or artificial cerebrospinal fluid for 7 days. To label proliferating cells, daily injections of thymidine analogues were administered. Proliferation was assessed in the PVRs of the medial wall of the lateral ventricles, the third ventricle, and the aqueduct/fourth ventricle (hindbrain).**

Results **Continuous VEGF-A infusion significantly increased overall cell proliferation in the third ventricle and hindbrain PVRs compared with controls, but not in the medial wall of the lateral ventricles. In hindbrain PVRs, the increase in proliferation was restricted to GFAP$^+$Sox2$^+$ NPCs. In contrast, in the wall of the third ventricle, VEGF-A infusion led to a significant reduction in ependymocyte proliferation, with no specific increase observed in other cell types.**

Conclusion **While continuous intracerebroventricular VEGF-A infusion enhances NPC proliferation in mid- and hindbrain PVRs, total counts of proliferating cells remain low, and significant lineage progression is not observed. These findings challenge the proposed neurorestorative role of resident NPCs in these brain regions, particularly in the context of neurodegenerative disorders such as Parkinson's disease.** ***NeuroReport*** **37: 722–730** **Copyright © 2026 The Author(s). Published by Wolters Kluwer Health, LLC.**

Graphical Abstract: ***https://links.lww.com/WNR/A873***

NeuroReport 2026, **37**:722–730

Keywords: adult neural stem cells, neural progenitor cells, neurorestoration, non-neurogenic regions, periventricular regions, vascular endothelial growth factor A

[a]Department of Neurology, University Medical Center Rostock, Rostock, Departments of [b]Neurology and [c]Psychotherapy and Psychosomatic Medicine, Faculty of Medicine and University Hospital Carl Gustav Carus, Technische Universität Dresden, Dresden, [d]Department of Neurology, Jena University Hospital, Jena, [e]German Centre for Neurodegenerative Diseases (DZNE) Rostock/Greifswald, [f]Translational Neurodegeneration Section 'Albrecht Kossel', Department of Neurology, [g]Center for Transdisciplinary Neurosciences Rostock (CTNR), Rostock University Medical Center, Rostock and [h]Department of Neurology and Neurogeriatrics, Medical School OWL, Klinikum Lippe, Bielefeld University, Lemgo, Germany

Correspondence to Mareike Fauser, MD, Department of Neurology, University Medical Center Rostock, Gehlsheimer Strasse 20, 18147 Rostock, Germany
Tel: +49 381 494 9668; fax: +49 381 494 4736;
e-mail: mareike.fauser@med.uni-rostock.de

*Mareike Fauser and Roy Bockholt contributed equally to the writing of this article and are co-first authors.

Received 4 June 2026 **Accepted** 4 September 2026.

Introduction

Adult neurogenesis is a well-characterized phenomenon that has initially been described in two discrete regions of the adult mammalian brain: the ventricular-subventricular zone (V-SVZ) of the lateral ventricular wall and the dentate gyrus of the hippocampus. The V-SVZ is composed of a hierarchically organized set of neural cell populations. Type B1 cells represent the bona fide neural stem cells (NSCs) within this niche; they maintain contact with local vasculature through specialized end-feet and coexpress astrocytic and stem cell markers, including glial fibrillary acidic protein (GFAP) and Sox2. Upon activation, B1 cells undergo self-renewal and generate rapidly dividing transit-amplifying progenitors (type C cells), which are characterized by epidermal growth factor receptor expression. These progenitors subsequently give rise to neuroblasts (type A cells) that express doublecortin (DCX) and polysialylated neural cell adhesion molecule and migrate along the rostral migratory stream to the olfactory bulb to differentiate into diverse interneuron subtypes [1]. In addition to neuronal turnover, the V-SVZ contributes to oligodendrogenesis, which is involved in myelin plasticity in the adult brain [2].

Supplemental Digital Content is available for this article. Direct URL citations appear in the printed text and are provided in the HTML and PDF versions of this article on the journal's website, www.neuroreport.com.

This is an open-access article distributed under the terms of the Creative Commons Attribution-Non Commercial-No Derivatives License 4.0 (CCBY-NC-ND), where it is permissible to download and share the work provided it is properly cited. The work cannot be changed in any way or used commercially without permission from the journal.

In humans, adult neurogenesis has been characterized much more recently. In the adult hippocampus, substantial neuronal turnover persists throughout life [3,4] and has been associated with maintaining cognitive function and emotional regulation [5]. Regarding V-SVZ neurogenesis, recent studies support a continuous turnover of striatal interneurons in humans [6].

The presence of adult NSCs has also been reported in various mammalian brain regions previously considered non-neurogenic, including the neocortex, striatum, hypothalamus, and substantia nigra [7]. It remains a matter of ongoing debate, however, whether these proliferating cells represent bona fide NSCs capable of long-term self-renewal, or rather, a more restricted progenitor cell population. Therefore, in this study, these cells will be referred to as neural progenitor cells (NPCs), in accordance with current literature conventions [8]. Our group and others have previously characterized resident adult NPCs (aNPCs) within the periventricular regions (PVRs) of the adult mouse brain [9–11]. In contrast to the V-SVZ, mid- and hindbrain PVRs lack a structured subependymal zone and are devoid of transit-amplifying progenitor cells or neuroblasts. While actively proliferating cells cannot be detected in these regions *in vivo*, aNPCs with proliferative capacity can be obtained from PVRs across the entire ventricular system *in vitro* [9]. Previously, we identified norepinephrine as a key negative regulator of these quiescent aNPCs. In the absence of norepinephrine, proliferating cells were detected *in vivo* within the third ventricle (3V)-PVR and surrounding the aqueduct. Yet, numbers of DCX^+ neuroblasts remained low, with the majority of proliferative activity occurring in $NG2^+$ glial cells [11].

Beyond its well-established role in angiogenesis [12], several in-vitro studies have demonstrated neuroprotective properties of VEGF [13,14]. In addition, vascular endothelial growth factor A (VEGF-A) has been shown to promote aNSC proliferation both *in vivo* and *in vitro* within the V-SVZ and dentate gyrus [15,16].

To date, VEGF effects on NPCs residing in mid- and hindbrain PVRs have not been systematically investigated. These NPCs remain mostly quiescent *in vivo* but possess the intrinsic capability to produce new neurons *in vitro* [9,10]. Therefore, they may represent a previously underexplored source of neurorestorative potential. In this study, a continuous intracerebroventricular infusion of VEGF-A or artificial cerebrospinal fluid (aCSF) was administered via osmotic minipumps over a period of 7 days in healthy young adult mice. The daily dose of VEGF-A (240 ng/day) was chosen according to the literature, using a dose regimen that promotes proliferation in the V-SVZ and dentate gyrus [15]. To label proliferating cells, daily intraperitoneal injections of thymidine analogues were performed. This approach enabled quantification of cell proliferation within the PVRs of the adult mouse brain, specifically in areas traditionally considered non-neurogenic.

Methods

Animals

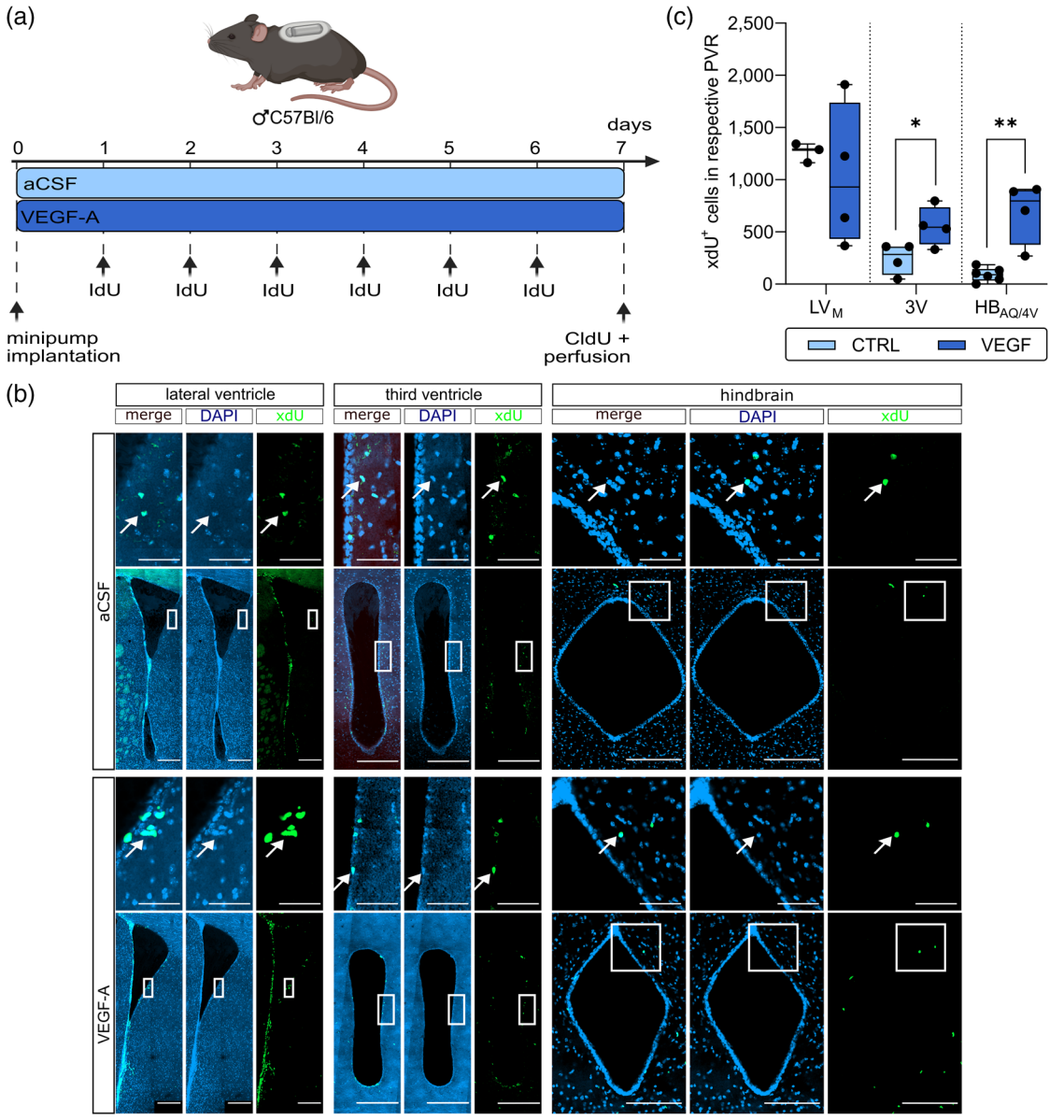
All procedures were permitted by responsible authorities (Thüringer Landesamt für Verbraucherschutz, Bad Langensalza, Thüringen, Germany; TVV 02-023/09) and carried out in line with Animal Research: Reporting of In Vivo Experiments (ARRIVE) guidelines and the European Union (EU) Directive 2010/63/EU. We used 12 male C57BL/J6 mice aged 8–12 weeks at the beginning of experiments.

Animals and surgery

For intracerebroventricular infusion, osmotic minipumps (flow rate 0.5 µL/h; total volume 100 µL; Durect Corporation, Cupertino, California, USA) were filled with either aCSF (Sigma-Aldrich, Gillingham, UK) or 20 µg/mL human $VEGF\text{-}A_{165}$ dissolved in aCSF (Sigma-Aldrich; 240 ng/day). This particular dose has been shown to promote proliferation in the V-SVZ and dentate gyrus [15]. Mice were placed in a stereotaxic frame (Stoelting Neuroscience, Dublin, Ireland) and anesthetized with isoflurane (5% for 1 min, then 2.5–3.5% with 0.8 L O_2/min; Baxter Deutschland GmbH, Unterschleißheim, Germany). A small incision was then made along the neck towards the left upper extremity to host the minipump. Subsequently, the skull was exposed, and a small burr hole was drilled at the following coordinates relative to the bregma and dura: anterior-posterior –0.5 mm; medial-lateral 1.3 mm, according to the study in Paxinos and Franklin [17]. The cannula of the infusion kit of the osmotic minipump (ALZET brain infusion kit 2; Durect Corporation) was then inserted to a depth of 2.5 mm into the right lateral ventricle and secured to the skull with dental cement as described earlier [11,18]. Before implantation, the osmotic minipumps were activated for 1 h in sterile saline at 37 °C as per the manufacturer's instructions. After surgery, animals were returned to their home cages and kept for another 7 days (see Fig. 1a for experimental setup).

To label proliferating NPCs, animals received daily (days 1–7) intraperitoneal injections of 5-iodo-2′-deoxyuridine (IdU; 57.5 mg/kg body weight; 23 mg/mL in 0.9% saline with 0.2 N NaOH; Sigma-Aldrich) and a single intraperitoneal dose of 5-chloro-2'-deoxyuridine (CldU; 42.5 mg/kg body weight; 17 mg/mL in 0.9% NaCl; MP Biochemicals, Santa Anna, California, USA) on the last day of the experiment. Initially, we had planned a separate quantification of IdU^+ and $CldU^+$ cells, but since proliferating cell counts in the PVRs were quite low, we chose a primary antibody that detected both IdU and CldU; proliferating cells are hereafter named xdU^+. At the end of the experiment, mice received an intraperitoneal overdose of ketamine/

Fig. 1



Experimental design and proliferating cell counts in the periventricular regions. (a) Experimental design. Male C57Bl/6 mice aged 8–12 weeks were implanted with osmotic minipumps loaded with either 20 µg/mL VEGF-A (240 ng/day) or aCSF, then received daily injections of IdU intraperitoneal for 6 days and a single dose of CldU immediately before perfusion. Figure created in BioRender. Fauser, M. (2026) https://BioRender.com/cjot7l0. (b) Representative immunofluorescence images of the medial wall of the lateral ventricles (left panel), third ventricle (middle panel), and hindbrain (aqueduct and fourth ventricle) after treatment with either aCSF (upper panel) or VEGF-A (lower panel). Examples of proliferating xdU (Idu+, CldU+, or both) cells (green) are indicated (white arrows), cell nuclei are counterstained with DAPI (blue). Scale bars, 200 µm and 50 µm, respectively. (c) After 7 days, continuous VEGF-A application into the lateral ventricles significantly increased xdU+ cell counts in the periventricular regions of the third ventricle ($P = 0.04$) and the hindbrain ($P = 0.001$); however, proliferation was not altered in the medial part of the lateral ventricles ($P = 0.60$). xdU+ cells were quantified in every sixth coronal section and results were multiplied by six. Data are presented as boxplots with a central mark at the median, bottom, and top edges of the boxes at the 25th and 75th percentiles, respectively, and whiskers at the minimum/maximum (dots represent individual values). *P* values are from Welch's t-test. 3V, third ventricle; aCSF, artificial cerebrospinal fluid; CldU, chlorodeoxyuridine; CTRL, control; DAPI, 4′,6-diamidino-2-phenylindole; HB, hindbrain (aqueduct + fourth ventricle); IdU, iododeoxyuridine; LVM, medial wall of the lateral ventricles; PVR, periventricular region; VEGF-A, vascular endothelial growth factor A.

xylazine [50 mg/kg body weight ketamine (Pfizer, New York, New York, USA) + 5 mg/kg body weight xylazine (Bayer Healthcare, Leverkusen, Germany)] and were perfused with ice-cold 0.9% saline, followed by 4% paraformaldehyde (PFA, Sigma-Aldrich). Brains were harvested, kept in 4% PFA overnight, transferred to a 30% sucrose solution, snap-frozen, and stored at −80 °C until further processing.

Immunofluorescence

Mouse brains were cut into 30-µm-thick coronal sections using a sliding microtome (SM2010R, Leica Microsystems, Germany) and stored at –20 °C until further processing. We chose the following coordinates for the different PVRs: 0.98–0.02 mm from bregma for medial wall of the lateral ventricles (LV_M), 0.02 to –2.7 mm for the 3V, –3.4 to –4.84 mm for the aqueduct, and –5.34 to –6.24 mm for the fourth ventricle (4V) [17]. Immunofluorescence was carried out essentially as described earlier [11]. In brief, free-floating cryo-sections (every sixth section) were preincubated in 1× tris-buffered saline (TBS; Dako, Germany) containing 3% donkey serum (Jackson ImmunoResearch, Ely, UK), and 0.2% Triton X-100 (Thermo Scientific, Waltham, Massachusetts, USA) for 30 min at room temperature (RT) and then incubated overnight at 4 °C with the following primary antibodies: sheep anti-BrdU for detection of IdU and CldU (1 : 250; RRID:AB_302659; Abcam, Cambridge, UK), goat anti-DCX (1 : 100; RRID:AB_2088491; Abcam), chicken anti-GFAP (1 : 1000; RRID: AB_2818977; Abcam), rabbit anti-NG2 chondroitin sulfate proteoglycan (1 : 200; RRID: AB_11213678; Merck Millipore, Burlington, Massachusetts, USA) and rabbit anti-Sox2 (1 : 200; RRID:AB_10585428; Abcam). The following day, sections were washed several times with 1× TBS and incubated with appropriate secondary fluorescence-conjugated antibodies for 1 h at RT (1 : 500; all from Molecular Probes, Eugene, Oregon, USA). For the detection of xdU incorporation, sections were incubated for 30 min in 2 N HCl at 37 °C before primary antibody application and were subsequently stained as described earlier. Cell nuclei were counterstained with 4′,6-diamidino-2-phenylindole (DAPI, Sigma-Aldrich).

Imaging and quantifications

Every sixth section of the V-SVZ, LV_M (contralateral to intracerebroventricular cannula), 3V, AQ, and 4V was analyzed using either a Zeiss Axioplan 2 (Carl Zeiss, Jena, Germany) and the optical fractionator method of the StereoInvestigator 7.50.4 software (MBF Bioscience, Williston, North Dakota, USA; for total counts of xdU^+ cells) or an Axio Observer Z1 with ZEN Blue Software (both from Carl Zeiss; for cell type analysis). Because of comparably low numbers of xdU^+ cells in the posterior PVRs, AQ and 4V were combined as hindbrain PVRs ($HB_{AQ/4V}$). Results were corrected for the total number of sections analyzed per brain region per animal. In each region, the PVR was defined as the region surrounding the ventricular wall by 200 µm as previously reported [9].

Statistics

All statistical analyses were performed using SPSS (version 29; IBM, Armonk, New York, USA). Data visualization, including plots and figures, was conducted using GraphPad Prism (version 9.4.1; GraphPad Software, San Diego, California, USA) and BioRender (BioRender.com; Toronto, Canada). Outliers were identified using the robust regression and outlier removal method. Normality of data distribution was evaluated with the Shapiro–Wilk test, and homogeneity of variances was assessed using Levene's test. Group differences in means or medians, respectively, were assessed using two-sided unpaired Student's t-tests, Welch's t-tests, or Mann–Whitney *U* tests, as appropriate. *P* values <0.05 were considered statistically significant.

Results

Vascular endothelial growth factor A increases proliferation in mid- and hindbrain periventricular regions of the adult mouse brain

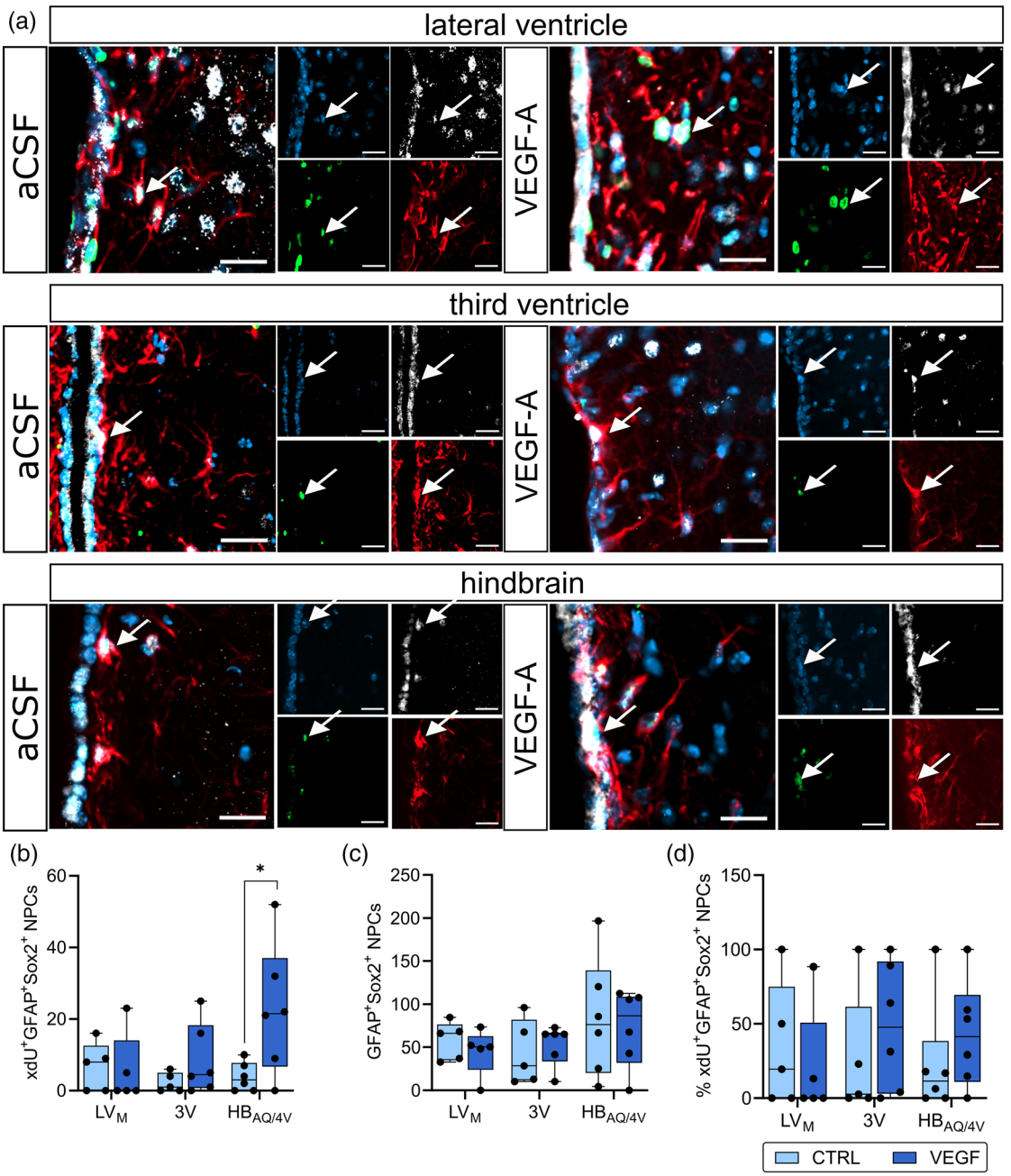
Since the present study aimed to investigate the effects of VEGF-A on cell proliferation within the so-called non-neurogenic PVRs, thymidine analog application was carried out daily to maximize the number of labeled NPCs, resulting in densely packed xdU^+ cells in the V-SVZ, which could not be reliably quantified anymore (see Fig. S1, Supplemental digital content 2, *https://links.lww.com/WNR/A874*). We evaluated the total number of proliferating cells – indicated by cumulative thymidine analogue incorporation – in the PVRs of the LV_M, 3V, and the hindbrain PVRs ($HB_{AQ/4V}$) following 7 days of continuous intracerebroventricular infusion of VEGF-A (240 ng/day) or aCSF (control). Animals received daily intraperitoneal injections of IdU (six in total) and a single injection of CldU the day before transcardial perfusion. Because of low numbers of proliferating cells in caudal PVRs, IdU^+ and $CldU^+$ cells were jointly quantified using a BrdU antibody that cross-reacts with both analogs, and the term xdU^+ cells was chosen (Fig. 1b).

In the LV_M, control animals exhibited 1265 ± 53 labeled cells, whereas VEGF-A-treated animals showed 1035 ± 343 cells ($P = 0.60$). In contrast, the 3V-PVR displayed a significant increase in xdU^+ cells in the VEGF-A group (555 ± 95) compared with controls (244 ± 74; $P = 0.04$). Similarly, analysis of the combined $HB_{AQ/4V}$ revealed a marked increase in proliferation in VEGF-A-treated animals (692 ± 148) relative to controls (90 ± 27; $P = 0.001$; Fig. 1c).

Effects of vascular endothelial growth factor A on neural progenitor cells and neuroblasts

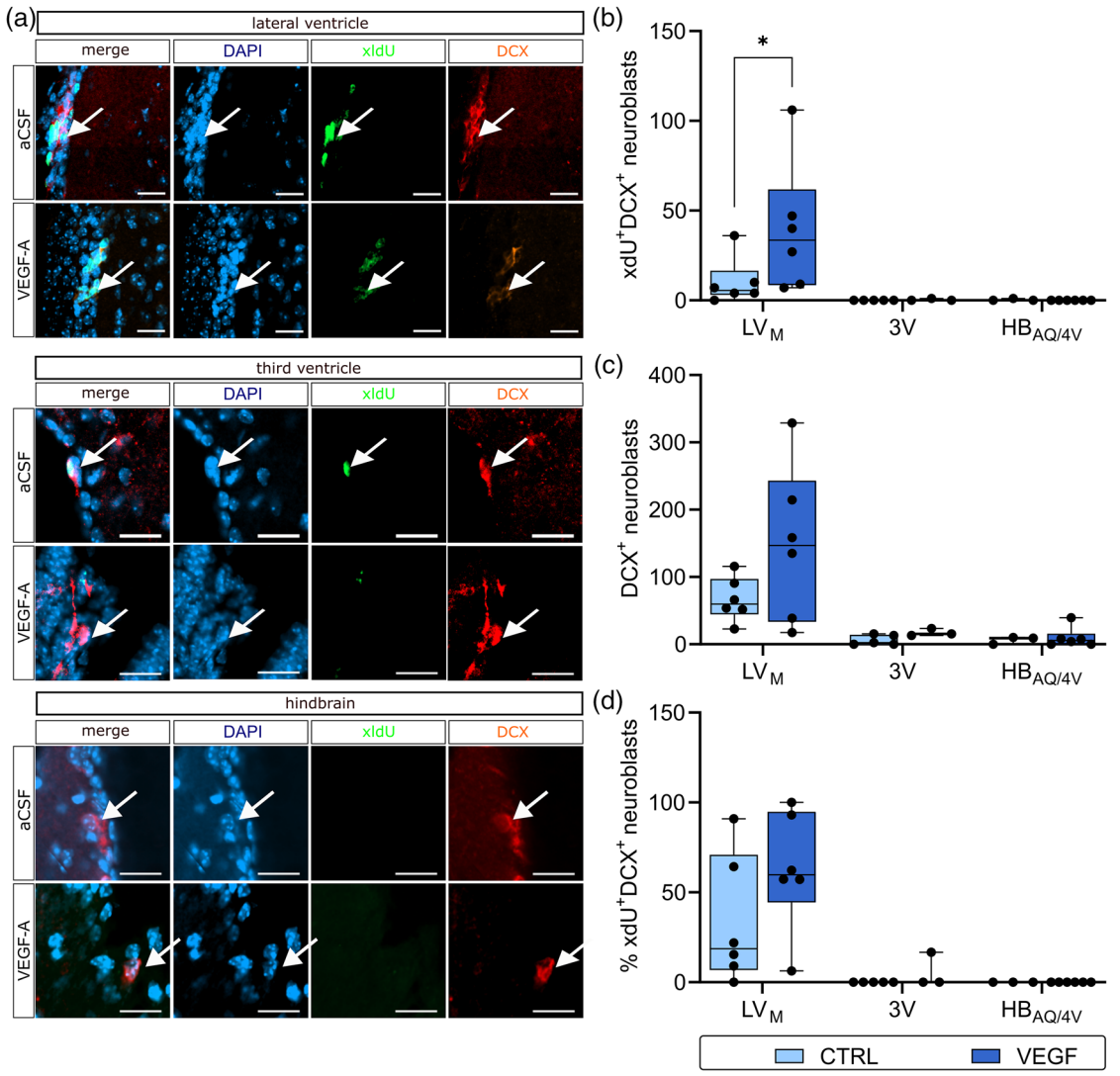
We next investigated whether VEGF-A specifically acts on certain cell types within the neurogenic cascade. After 7 days, VEGF-A did not alter the proliferation of $GFAP^+Sox2^+$ NPCs in the LV_M (7 ± 3 vs. 6 ± 4 cells; $P = 0.29$) or the 3V (2 ± 1 vs. 9 ± 4 cells; $P = 0.19$), but significantly increased proliferation in the $HB_{AQ/4V}$ (4 ± 2 vs. 23 ± 7 cells; $P = 0.03$; Fig. 2a, b). In addition, VEGF-A did not influence the absolute numbers of (nonproliferating) $GFAP^+Sox2^+$ NPCs across the examined regions with the following cell counts: LV_M (control vs. VEGF-A), 58 ± 10

Fig. 2



Effects of VEGF-A on neural progenitor cells in the periventricular regions. (a) Representative immunofluorescence images of the medial wall of the lateral ventricles (upper panel), third ventricle (middle panel), and hindbrain PVRs (aqueduct and fourth ventricle; lower panel) after continuous intracerebroventricular treatment with either aCSF (control condition, left panel) or VEGF-A (right panel) for 7 days. Immunfluorescence identifies xdU (IdU, CldU, or both; green), Sox2 (white), and GFAP (red); cell nuclei are counterstained with DAPI (blue). Marker-positive cells are indicated with white arrows. Scale bars, 20 µm. (b) Compared with controls, continuous intraventricular VEGF-A infusion increased numbers of xdU$^+$GFAP$^+$Sox2$^+$ NPCs in hindbrain PVRs ($HB_{AQ/4V}$; $P = 0.03$); however, proliferation in the medial wall of the lateral ventricles and the third ventricle, respectively, remained unchanged. (c) Compared with controls, continuous intraventricular VEGF-A infusion did not alter GFAP$^+$Sox2$^+$ NPCs counts in the medial wall of the lateral ventricles, the third ventricle and the hindbrain regions. (d) The percentage of xdU$^+$GFAP$^+$Sox2$^+$ NPCs was not altered in any of the examined PVRs. GFAP$^+$Sox2$^+$ NPCs were quantified in every sixth coronal section and results were multiplied by six. Data are presented as boxplots with a central mark at the median, bottom, and top edges of the boxes at the 25th and 75th percentiles, respectively, and whiskers at the minimum/maximum (dots represent individual values). *P* values are from Welch's t-test. 3V, third ventricle; aCSF, artificial cerebrospinal fluid; CldU, chlorodeoxyuridine; CTRL, control; DAPI, 4′,6-diamidino-2-phenylindole; GFAP, glial fibrillary acidic protein; HB, hindbrain (aqueduct + fourth ventricle); IdU, iododeoxyuridine; LVM, medial wall of the lateral ventricles; NPC, neural progenitor cell; PVR, periventricular region; VEGF-A, vascular endothelial growth factor A.

Fig. 3

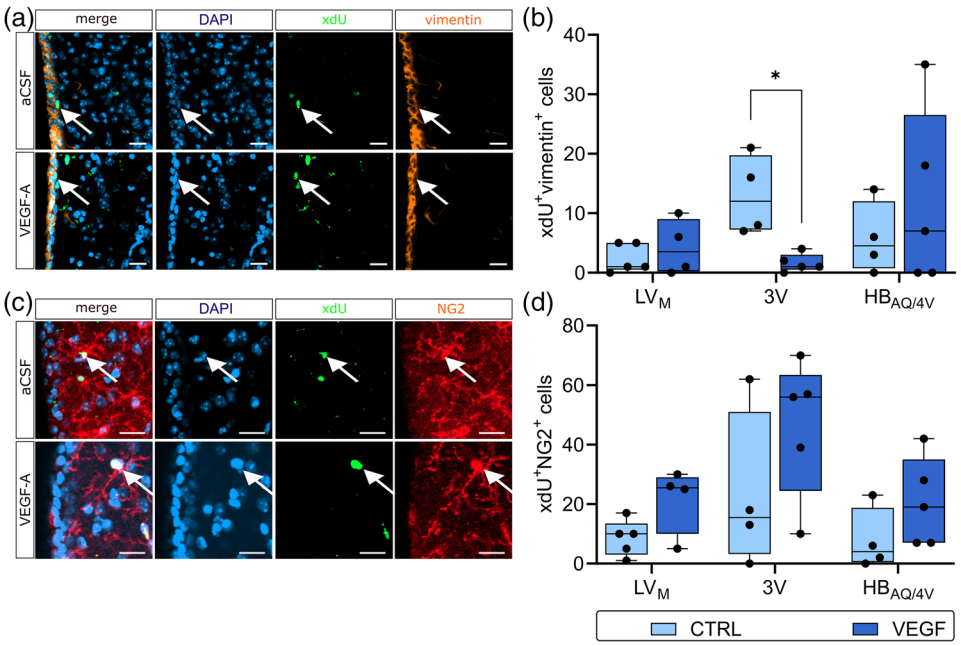


Effects of VEGF-A on neuroblasts in the periventricular regions. (a) Representative immunofluorescence images of the LV_M (upper panel), third ventricle (middle panel), and hindbrain (aqueduct and fourth ventricle; lower panel) to identify xdU (Idu+, CldU+, or both) cells (green) and DCX+ neuroblasts (orange); cell nuclei are counterstained with DAPI (blue). Scale bars, 20 μm. (b) Compared with controls, continuous intracerebroventricular VEGF-A infusion significantly increased total numbers of xdU+ DCX+ neuroblasts in the medial wall of the lateral ventricles ($P = 0.02$), but not in mid- and hindbrain PVRs. (c) Compared with controls, continuous intraventricular VEGF-A infusion did not alter total numbers of DCX+ neuroblasts in the medial wall of the lateral ventricles, the third ventricle, and the hindbrain periventricular regions. (d) The percentage of xdU+GFAP+Sox2+ NPCs was not altered in any of the examined PVRs. DCX+ neuroblasts were quantified in every sixth coronal section and results were multiplied by six. Data are presented as boxplots with a central mark at the median, bottom, and top edges of the boxes at 25th and 75th percentiles, respectively, and whiskers at the minimum/maximum (dots represent individual values). *P* values are from Welch's t-test. $*P < 0.05$. 3V, third ventricle; aCSF, artificial cerebrospinal fluid; CldU, chlorodeoxyuridine; CTRL, control; DAPI, 4′,6-diamidino-2-phenylindole; GFAP, glial filament-associated protein; HB, hindbrain (aqueduct + fourth ventricle); IdU, iododeoxyuridine; LVM, medial wall of the lateral ventricles; VEGF-A, vascular endothelial growth factor A.

vs. 45 ± 12 ($P = 0.43$); 3V, 43 ± 17 vs. 53 ± 10 ($P = 0.79$); $HB_{AQ/4V}$, 83 ± 28 vs. 73 ± 18 ($P = 0.76$; Fig. 2c). The fraction of xdU+GFAP+Sox2+ NPCs (% xdU+GFAP+Sox2+ NPCs/total GFAP+Sox2+ NPCs) also remained unchanged in any of the examined PVRs (Fig. 2d).

Lineage progression was assessed in neuroblasts, with significantly higher numbers of xdU+DCX+ proliferating neuroblasts in the LV_M of VEGF-A-treated animals compared with controls (10 ± 5 vs. 40 ± 15 cells; $P = 0.02$), while no differences were observed in the 3V (0 ± 0 vs. 0.3 ± 0.3 cells; $P = 0.57$) or $HB_{AQ/4V}$ (0.3 ± 0.3 vs. 0 ± 0 cells; $P = 0.55$; Fig. 3a, b). Moreover, no significant differences were observed in the total number of DCX+ neuroblasts: LV_M, 67 ± 13 vs. 149 ± 47 ($P = 0.12$); 3V, 6 ± 3 vs. 17 ± 3 ($P = 0.07$); $HB_{AQ/4V}$, 6 ± 3 vs. 4 ± 2 ($P = 0.71$; Fig. 3c). As for GFAP+Sox2+ NPCs, the percentage of xdU+DCX+ neuroblasts (to total DCX+

Fig. 4



Effects of VEGF-A on vimentin+ ependymocytes and NG2+ oligodendroglial precursor cells in the periventricular regions. (a) Representative immunofluorescence stainings of the medial wall of the lateral ventricle to identify xdU (Idu+, CldU+, or both) cells (green) and vimentin+ ependymocytes (orange); cell nuclei are counterstained with DAPI (blue). Scale bars, 20 µm. (b) Continuous intraventricular VEGF-A infusion significantly decreased xdU+vimentin+ ependymocytes exclusively in the periventricular region of the third ventricle, but not in the other periventricular regions. (c) Representative immunofluorescence stainings of the medial wall of the lateral ventricle to identify xdU+ cells (green) and NG2+ oligodendrocyte progenitor cells (orange); cell nuclei are counterstained with DAPI (blue). Scale bars, 20 µm. (d) Numbers of xdU+NG2+ oligodendroglial precursor cells were not altered after 8 days of VEGF-A infusion compared with controls in any periventricular region. Ependymocytes and oligodendroglial precursor cells were quantified in every sixth coronal section and results were multiplied by six. Data are presented as boxplots with a central mark at the median, bottom, and top edges of the boxes at 25th and 75th percentiles, respectively, and whiskers at the minimum/maximum (dots represent individual values). *P* values are from Welch's t-test. 3V, third ventricle; aCSF, artificial cerebrospinal fluid; CldU, chlorodeoxyuridine; CTRL, control; DAPI, 4′,6-diamidino-2-phenylindole; HB, hindbrain (aqueduct + fourth ventricle); IdU, iododeoxyuridine; LVM, medial wall of the lateral ventricles; VEGF-A, vascular endothelial growth factor A.

neuroblasts) was not affected by VEGF-A treatment (Fig. 3d).

In ancillary analyses, we determined the effects of VEGF-A on the proliferation of vimentin+ ependymocytes. In the LV_M, 2 ± 1 and 4 ± 2 xdU+vimentin+ ependymocytes were detected in control and VEGF-A-treated animals, respectively ($P = 0.46$). In the 3V, VEGF-A significantly reduced proliferation (13 ± 3 vs. 2 ± 1 cells, $P = 0.04$), while in $HB_{AQ/4V}$ no significant difference was observed (6 ± 3 vs. 12 ± 7 cells, $P = 0.46$; Fig. 4a, b).

Finally, analysis of NG2+ oligodendroglial progenitor cells showed a trend toward increased proliferation with VEGF-A in the LV_M (9 ± 3 vs. 22 ± 6 cells; $P = 0.06$) without altered proliferation in the 3V (23 ± 13 vs. 46 ± 10 cells; $P = 0.21$) and $HB_{AQ/4V}$ (8 ± 5 vs. 21 ± 7 cells; $P = 0.19$; Fig. 4c, d).

Discussion

The present study provides the first evidence that VEGF-A promotes NPC proliferation in mid- and hindbrain PVRs of the adult mouse brain, which are traditionally considered non-neurogenic regions of the periventricular system. We previously demonstrated that these PVRs differ markedly from the V-SVZ of the lateral ventricles with respect to their structural organization and absence of actively proliferating cells *in vivo* under physiological conditions despite retaining cell populations with proliferative potential *in vitro* [9]. In contrast to these earlier findings, the present study revealed low numbers of proliferating cells in all PVRs *in vivo*, even under control conditions. This discrepancy may be attributable to the extended thymidine analog administration used here (7 days vs. 3 days). In addition to GFAP+Sox2+ NPCs, we detected few DCX+ neuroblasts in all PVRs, although in very low numbers.

VEGF-A treatment significantly increased total cell proliferation in the mid- and hindbrain PVRs, but not in the LV_M. Analysis of cell fate revealed a significant increase in xdU+DCX+ neuroblasts within the forebrain PVR of the LV_M, consistent with enhanced lineage progression rather than a primary effect on proliferation. In hindbrain PVRs, VEGF-A selectively promoted the

proliferation of GFAP$^+$Sox2$^+$ NPCs without evidence of downstream lineage progression, as indicated by the near absence of xdU$^+$DCX$^+$ neuroblasts. Around the 3V, VEGF-A treatment increased cell proliferation; however, the identity of the targeted cell population(s) could not be conclusively determined. Notably, in a previous study, we demonstrated that norepinephrine significantly suppresses the proliferative capacity of caudal NPCs *in vivo*. Pharmacological antagonism of norepinephrine signaling led to increased proliferation across multiple stages of the neurogenic lineage – including NPCs, neuroblasts, and oligodendrocyte progenitors – around the 3V, without affecting tanycyte proliferation [11]. Collectively, these findings indicate that VEGF-A exerts region-specific effects on distinct precursor cell populations within the adult periventricular system. This regional heterogeneity underscores the need for further investigation into the mechanisms underlying VEGF-A-mediated regulation of proliferation in these niches.

Previous studies demonstrated dose-dependent effects of VEGF-A, with higher doses of 240 ng/day (as used here) resulting in increased V-SVZ-aNSCs proliferation compared with low-dose regimens (2.4 ng/day) [15,16]. Notably, the latter study also reported a predominant VEGF-A influence on survival, an aspect not addressed in the present investigation. As indicated earlier, because of prolonged VEGF-A infusion (7 days) and consistent with previous protocols [17], we were unable to quantify xdU-labeled cells in the V-SVZ, as the region became densely populated with immunopositive cells. As a resulting limitation, direct within-animal comparisons of VEGF-A effects across V-SVZ and mid-/hindbrain PVRs were unfortunately not feasible. While hypoxia and ischemia are established modulators of V-SVZ neurogenesis [19], equivalent regulators in mid- and hindbrain PVRs, which might have been of additional interest in our study, remain poorly defined.

Limitations of this study include the small sample size, although comparable to those in related work [15,16], and the exclusive use of male mice. Given that sex hormones are known to influence VEGF signaling and neurogenesis [20], this restricts the generalizability of our findings, although we can exclude confounding influences of the female hormonal cycle on NPC proliferation. In addition, we did not assess VEGF-A kinetics in the CSF in hindbrain regions distant from the infusion site. Our study did not analyze proliferation of transit-amplifying cells, which may partly account for altered counts of proliferating cells. Moreover, we cannot provide data on VEGF-A effects on endothelial cells or vascular remodeling, which could indirectly influence neurogenesis in the PVRs. As already discussed above, the repeated application of thymidine analogues prevented the quantification of VEGF-A effects on V-SVZ aNSC proliferation in a 'traditional' neurogenic niche.

In summary, our findings provide initial evidence that VEGF-A enhances proliferation in mid- and hindbrain PVRs beyond the V-SVZ. The overall low number of proliferating cells, however, raises questions about the therapeutic relevance of our results. Future studies should explore detailed lineage progression and functional integration of newly generated cells in the PVRs, as well as VEGF-A influences on vascularization.

Acknowledgements

This work was supported by the Deutsche Forschungsgemeinschaft (DFG) through the Collaborative Research Centre CRC 1270 'Electrically Active Implants' (DFG; SFB 1270/1,2,3 – 299150580) to A.S. and M.F.; M.F. was supported by the Else Hirschberg Women's Advancement Program of the University Medical Center Rostock and a research grant from the Deutsche Gesellschaft für Parkinson und Bewegungsstörungen (DPG). A.H. was supported by the Hermann and Lilly Schilling Stiftung für medizinische Forschung im Stifterverband.

M.F. contributed in formal analysis and writing – original draft. R.B. contributed in investigation and formal analysis. S.K. contributed in investigation and writing – review & editing. G.W. contributed in investigation and formal analysis. C.R. contributed in conceptualization, funding acquisition, and writing – review & editing. A.H. contributed in supervision, funding acquisition, and writing – review & editing. A.S. contributed in conceptualization, supervision, funding acquisition, and writing – review & editing.

The data used to support the findings of this study are available from the corresponding author upon request.

All animal experiments adhered to the European Directive (2010/63/EU) and ARRIVE guidelines and were approved by the local animal care committee.

All authors read and approved the final manuscript.
R.B. included these data in his doctoral thesis.

Conflicts of interest

There are no conflicts of interest.

References

1 Fuentealba LC, Rompani SB, Parraguez JI, Obernier K, Romero R, Cepko CL, Alvarez-Buylla A. Embryonic origin of postnatal neural stem cells. *Cell* 2015; **161**:1644–1655.
2 Radecki DZ, Samanta J. Endogenous neural stem cell mediated oligodendrogenesis in the adult mammalian brain. *Cells* 2022; **11**:2101.
3 Dumitru I, Paterlini M, Zamboni M, Ziegenhain C, Giatrellis S, Saghaleyni R, *et al*. Identification of proliferating neural progenitors in the adult human hippocampus. *Science* 2025; **389**:58–63.
4 Spalding KL, Bergmann O, Alkass K, Bernard S, Salehpour M, Huttner HB, *et al*. Dynamics of hippocampal neurogenesis in adult humans. *Cell* 2013; **153**:1219–1227.
5 Moreno-Jiménez EP, Flor-García M, Terreros-Roncal J, Rábano A, Cafini F, Pallas-Bazarra N, *et al*. Adult hippocampal neurogenesis is abundant in neurologically healthy subjects and drops sharply in patients with Alzheimer's disease. *Nat Med* 2019; **25**:554–560.

6 Ernst A, Alkass K, Bernard S, Salehpour M, Perl S, Tisdale J, *et al*. Neurogenesis in the striatum of the adult human brain. *Cell* 2014; **156**:1072–1083.
7 Martino G, Butti E, Bacigaluppi M. Neurogenesis or non-neurogenesis: that is the question. *J Clin Invest* 2014; **124**:970–973.
8 Bonfanti L, Peretto P. Adult neurogenesis in mammals – a theme with many variations. *Eur J Neurosci* 2011; **34**:930–950.
9 Hermann A, Suess C, Fauser M, Kanzler S, Witt M, Fabel K, *et al*. Rostro-caudal gradual loss of cellular diversity within the periventricular regions of the ventricular system. *Stem Cells* 2009; **27**:928–941.
10 Golmohammadi MG, Blackmore DG, Large B, Azari H, Esfandiary E, Paxinos G, *et al*. Comparative analysis of the frequency and distribution of stem and progenitor cells in the adult mouse brain. *Stem Cells* 2008; **26**:979–987.
11 Weselek G, Keiner S, Fauser M, Wagenführ L, Müller J, Kaltschmidt B, *et al*. Norepinephrine is a negative regulator of the adult periventricular neural stem cell niche. *Stem Cells* 2020; **38**:1188–1201.
12 Plouët J, Schilling J, Gospodarowicz D. Isolation and characterization of a newly identified endothelial cell mitogen produced by AtT-20 cells. *EMBO J* 1989; **8**:3801–3806.
13 Jin KL, Mao XO, Greenberg DA. Vascular endothelial growth factor rescues HN33 neural cells from death induced by serum withdrawal. *J Mol Neurosci* 2000; **14**:197–203.
14 Silverman WF, Krum JM, Mani N, Rosenstein JM. Vascular, glial and neuronal effects of vascular endothelial growth factor in mesencephalic explant cultures. *Neuroscience* 1999; **90**:1529–1541.
15 Jin K, Zhu Y, Sun Y, Mao XO, Xie L, Greenberg DA. Vascular endothelial growth factor (VEGF) stimulates neurogenesis in vitro and in vivo. *Proc Natl Acad Sci U S A* 2002; **99**:11946–11950.
16 Schänzer A, Wachs F-P, Wilhelm D, Acker T, Cooper-Kuhn C, Beck H, *et al*. Direct stimulation of adult neural stem cells in vitro and neurogenesis in vivo by vascular endothelial growth factor. *Brain Pathol* 2004; **14**:237–248.
17 Paxinos G, Franklin KBJ. *Paxinos and Franklin's the mouse brain in stereotaxic coordinates*. 5th ed. Academic Press; 2019.
18 Keiner S, Witte OW, Redecker C. Immunocytochemical detection of newly generated neurons in the perilesional area of cortical infarcts after intraventricular application of brain-derived neurotrophic factor. *J Neuropathol Exp Neurol* 2009; **68**:83–93.
19 Ceanga M, Dahab M, Witte OW, Keiner S. Adult neurogenesis and stroke: a tale of two neurogenic niches. *Front Neurosci* 2021; **15**:700297.
20 Collignon A, Dion-Albert L, Ménard C, Coelho-Santos V. Sex, hormones and cerebrovascular function: from development to disorder. *Fluids Barriers CNS* 2024; **21**:2.